

Numerical simulation of the constructive steps of a cable-stayed bridge using ANSYS

Paula M. Lazzari^{*1}, Américo Campos Filho¹, Bruna M. Lazzari¹,
Alexandre R. Pacheco¹ and Renan R. S. Gomes²

¹Civil Engineering Graduate Program, Federal University of Rio Grande do Sul, 99 Oswaldo Aranha Ave, 90035-190, Porto Alegre, RS, Brazil

²Civil Engineering Graduate Program, Federal University of Rio de Janeiro, 550 Pedro Calmon Ave, 21941-901, Rio de Janeiro, RJ, Brazil

(Received January 23, 2018, Revised May 20, 2018, Accepted May 21, 2018)

Abstract. This work addresses a three-dimensional nonlinear structural analysis of the constructive phases of a cable-stayed segmental concrete bridge using The Finite Element Method through ANSYS, version 14.5. New subroutines have been added to ANSYS via its UPF customization tool to implement viscoelastoplastic constitutive equations with cracking capability to model concrete's structural behavior. This numerical implementation allowed the use of three-dimensional twenty-node quadratic elements (SOLID186) with the Element-Embedded Rebar model option (REINF264), conducting to a fast and efficient solution. These advantages are of fundamental importance when large structures, such as bridges, are modeled, since an increasing number of finite elements is demanded. After validating the subroutines, the bridge located in Rio de Janeiro, Brazil, and known as "Ponte do Saber" (Bridge of Knowledge, in Portuguese), has been numerically modeled, simulating each of the constructive phases of the bridge. Additionally, the data obtained numerically is compared with the field data collected from monitoring conducted during the construction of the bridge, showing good agreement.

Keywords: cable-stayed bridges; bridge modeling; numerical analysis; the Finite Element Method; ANSYS; the UPF customization tool

1. Introduction

The number of stayed-cable bridges has increased in the last years, since this type of bridge is an interesting alternative for large spans. It makes it possible to build lighter, slender, and less expensive structures. Nevertheless, this type of bridge tends to be sensitive to the constructive sequence and, therefore, a deep understanding of its structural behavior becomes of fundamental importance.

Still during the designing process, numerical simulations of the constructive phases accounting for complex conditions can be carried out to follow the evolution of stresses and displacements that occur in the bridge's structural components. In this way, a complete understanding of the structural behavior along the constructive phases of the bridge can be reached, avoiding potential problems that could appear during the construction.

In that context, this work presents a complex numerical analysis based on the Finite Element Method (FEM) of the structural behavior of a cable-stayed segmental bridge during its constructive steps. The bridge was erected through the cast in place segmental cantilever method, with the segment casting occurring simultaneously to the cable-stay prestressing.

Although not specific for bridge designs, but more of a general FEM purpose program, ANSYS, in its 14.5 version, has been the modeling tool chosen for simulation. ANSYS is very well established in industry and the research sector mainly because of its constant development and a variety of alternatives in terms of element types and constitutive models. However, in order to simulate numerically a real bridge with great precision regarding material behavior, it has been necessary to implement new constitutive models for the concrete and for the steel. Additionally, a great advantage in terms of solution efficiency can be taken by adopting the Element-Embedded Rebar option available in ANSYS.

Among recent studies that can be cited as using the FEM to analyze bridges, there is the work by Mondal and Prakash (2016) that created a nonlinear finite element model to analyze the behavior of reinforced concrete bridge piers under combined states of compression and torsion. Also, worth mentioning, there is the work by Zhu *et al.* (2015) that used the FEM to evaluate effectively the performance and safety of cable-stayed bridges studying in detail the structural elements of the Stonecutters Bridge, in Hong Kong. Others studies on concrete structures using ANSYS are also found in the works of Kazaz (2011), Bulut

*Corresponding author, Professor
E-mail: p.manica.lazzari@gmail.com

^aProfessor
E-mail: americo@ufrgs.br

^bPh.D. Student
E-mail: bruna.ml@gmail.com

^cProfessor
E-mail: apacheco@ufrgs.br

^dPh.D. Student
E-mail: rgomes@queirozgalvao.com

et al. (2011), Amiri et al. (2012), Anil and Uyaroglu (2013), Kibar and Ozturk (2014), Demir et al. (2014), Demir and Husem (2015), Adiyaman et al. (2015) and Shaheen et al. (2016).

The numerical model developed for this work to simulate the viscoelastoplastic behavior of the concrete and the reinforcement of the bridge analyzed, has been implemented through the customization tool UPF (User Programmable Features) of ANSYS, adding new subroutines written in FORTRAN to the main subroutine (USERMAT). These newly implemented subroutines have been validated in simulations of sixteen reinforced concrete beams originally lab tested by Leonhardt and Walther (1962), and by Bresler and Scordelis (1963). Additionally, the data from a prestressed segmental box girder tested by Aparicio et al. (2002) were also considered to validate the subroutines. All these comparisons and validations are given in detail in the PhD dissertation by Lazzari (2016) and in Lazzari et al (2017b) with additional verifications also for plane stress states in Lazzari (2015) and Lazzari et al. (2017a).

2. Constitutive models

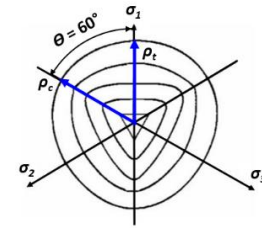
Since structural concrete behaves in a complex manner, a deep understanding of the properties of its compound materials is of fundamental importance. Additionally, in this case, the constitutive equations of materials, relating stresses, strains, and time, are also fundamental when a more precise and detailed analysis is intended, mainly when strong nonlinear behaviors are present.

In this work, the behavior of structural concrete is based on two different constitutive models. The first one is an elastoplastic model for instantaneous responses, while a second one, a viscoelastic model, deals with the responses that are affected by time. Thus, these two models are used together, but during increments of different variables. The elastoplastic model works during load increments, with the viscoelastic one working during the increments of time.

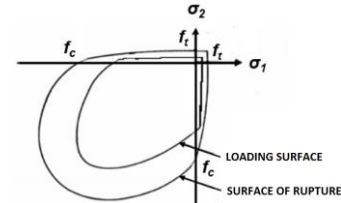
Regarding the reinforcement, typical simplifications and considerations are adopted for the steel rebars, i.e., they are considered to transmit only axial forces and present the same response either in compression or in tension. The mechanical behavior of the steel rebars is represented by a bilinear stress-strain diagram.

2.1 Constitutive models for concrete

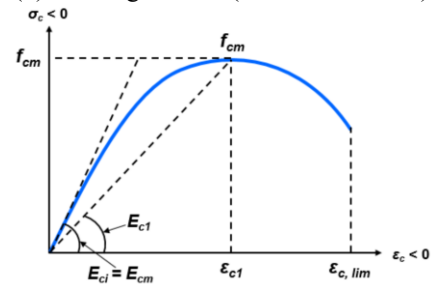
One of the main characteristics of how concrete behaves mechanically is its low strength in tension, when compared with a high strength under compression. Therefore, two distinct models are used herein to simulate these responses. An elastoplastic model with hardening is employed for the concrete under compression, while a linear elastic consideration is used for the tensioned concrete. Additionally, during a tensile loading, up to the rupture of the concrete, the tension stiffening effect is evaluated, measuring the stress contribution of the material between cracks.



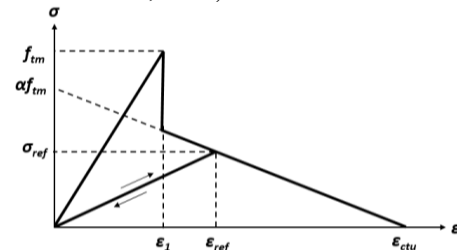
(a) Rupture surface (CHEN and HAN 1988)



(b) Loading surface (OTTOSEN 1977)



(c) Stress-strain curve for compressed concrete (*fib* MODEL CODE 2010, 2012)



(d) Stress-strain relation for tensioned concrete (HINTON 1988)

Fig. 1 Models for the compressed and tensioned concrete

The model for the compressed concrete is composed by a rupture criterion, a plastification criterion, and a hardening rule. The model by Ottosen (1977) is used as the rupture criterion, since it is currently adopted by *fib* Model Code 2010 (2012). Cross-sections of the rupture surface in a three-dimensional stress space is shown in Fig. 1(a). It is considered that the compressed concrete has isotropic hardening and, therefore, its loading surfaces have the same shape of its rupture surface. These surfaces are schematically shown in Fig. 1(b). The hardening rule, which is described by the effective plastic stress-strain relation, defines how loading surfaces move during plastic deformation. The hardening rule can be used to extrapolate from simple uniaxial test results to multiaxial state conditions. The stress-strain diagram used is shown in Fig. 1(c), which is also recommended by *fib* Model Code 2010 (2012).

Concrete under tensile stresses is modeled as an elastic material with softening. Before cracking, it behaves linear

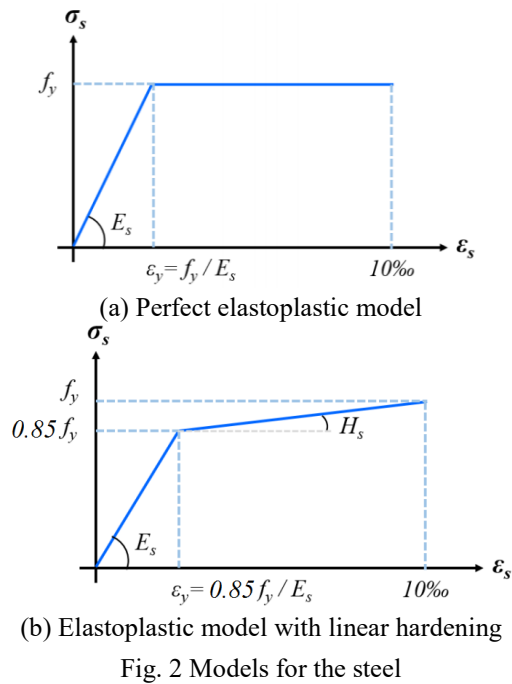


Fig. 2 Models for the steel

elastically and, when cracking takes place, a smeared cracking model with tension stiffening is used, as indicated in Fig. 1(d). The cracking model used, which considers a cracking criterion, a collaboration rule for the concrete between cracks, and a shear-locking model, is based on the formulation presented by Hinton (1988).

2.2 Constitutive models for steel

The reinforcing bars follow two behaviors, depending upon the fabrication process considered. A perfect elastoplastic model is adopted for steels with a well-defined yield plateau, while a variation with linear hardening after 85% of the yield stress, f_y , is used for cold rolled cases. The stress-strain diagrams for both cases are shown in Fig. 2.

The behavior adopted for the prestressing reinforcement is similar to the one considered for cold rolled steels, but with a linear elastic response up to 90% of the rupture stress, f_{ptk} . Upon reaching this value, a linear hardening is also considered in this case.

3. Time dependent material properties

Time dependent effects, such as creep and shrinkage of concrete and relaxation of prestressing steel, significantly influence, most of the time in a negative way, the behavior of structural concrete. These effects tend to be more prominent in structures that present a long construction schedule, as typically occurs with bridges. Therefore, these effects have to be considered when more real and precise results are demanded. Regarding concrete, creep and shrinkage strains have the same order of magnitude as instantaneous ones, due to the stress levels that are typically observed. Additionally, regarding prestressing reinforcement, relaxation effects generate a considerable stress loss with time, which therefore should be accounted

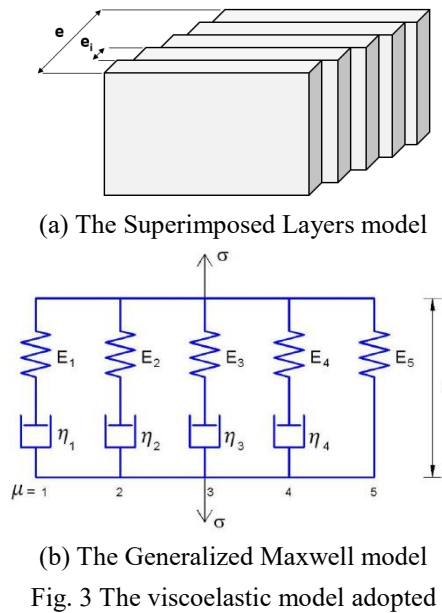


Fig. 3 The viscoelastic model adopted

for.

It is possible to use a viscoelastic model to represent both immediate and time dependent strains. Instantaneous strains are dealt by the elastic part of the model, simultaneously dealing with corresponding stresses without any variation in time. Time dependent strains, however, are dealt by the viscous part of the model, varying in time upon application of a certain load to the material.

The ageing process is considered through a set of five Maxwell elements arranged in parallel, with each element composed by two rheological basic elements connected in series: an elastic spring and a viscous dashpot. This set of Maxwell elements characterizes the Superimposed Layers model adopted, where each layer is represented by one of the Maxwell elements of the set. Each layer of the model has its own thickness and set of mechanical properties, allowing the simulation of the overall complex behavior of concrete. The layers are always subjected to the same total strain, but each one contributes with its own share of stress, relatively to its thickness, e_i . In Figs. 3(a) and 3(b) are represented respectively both the Superimposed Layers model and the chain of five Maxwell elements associated in parallel, which is also known as the Generalized Maxwell model.

The determination of the parameters for creep and shrinkage functions of the concrete and for relaxation of the prestressing reinforcement has been carried out accordingly with the recommendations given by the *fib* Model Code 2010 (2012).

4. Computational model

The Finite Element Method (FEM) is the approach chosen to simulate numerically the constructive phases of the cable-stayed bridge analyzed. Through FEM, it is possible to consider the strong nonlinear behavior of both concrete and steel, including processes such as cracking in concrete and plastification in both materials.

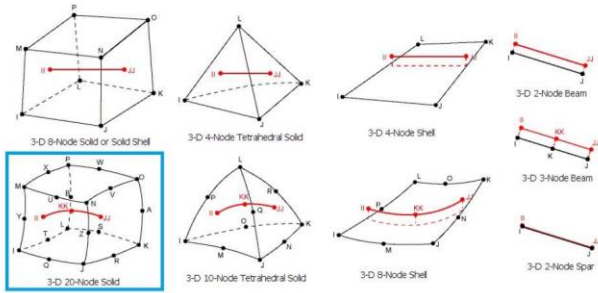


Fig. 4 Compatibility of element REINF264 with other elements (ANSYS 2013)

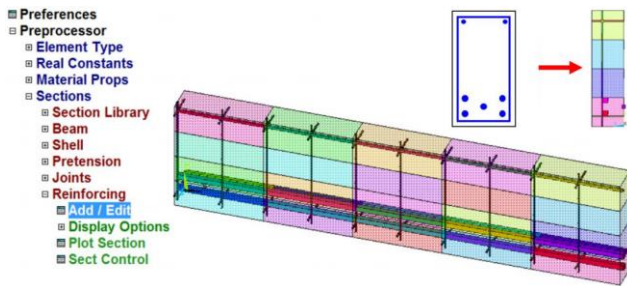


Fig. 5 Example of discretization with element REINF264

Program ANSYS, a powerful option for research, in its 14.5 version, has been chosen as the tool for creating the numerical model of this study. ANSYS is a platform that, besides offering a number of finite element options and constitutive models, also offers its UPF customization tool (User Programmable Features). Through this valuable capability, implementations of new material models and new finite elements can be carried out for specific purposes. In this work, FORTRAN programming language has been used for creating new models for the materials, using finite elements that allow the Element-Embedded model for discretization of the reinforcement.

4.1 Finite elements used

The finite element SOLID186, a known element that is listed in ANSYS library, is used to model concrete. SOLID186 is a three-dimensional twenty-node quadratic element that has three degrees of freedom per node, corresponding to the translations in X, Y, and Z directions. Besides its hexahedral base configuration, the element can have pyramidal, prismatic, or tetrahedral configurations, facilitating adjustments to complex geometries. SOLID186 has been chosen because of its good results with relatively coarse meshes, drastically contributing with the reduction in processing time during a structural analysis. Another aspect that had to be taken into consideration when choosing the element type was its compatibility with element REINF264, which has been picked for the reinforcement. Therefore, a discrete representation of the reinforcement, rather than a smeared approach, has been considered for a more realistic simulation of the structure analyzed.

Element REINF264 can be used together with a variety of element types, such as bars, plates, shells, or solids. This element is adequate for simulating randomly oriented

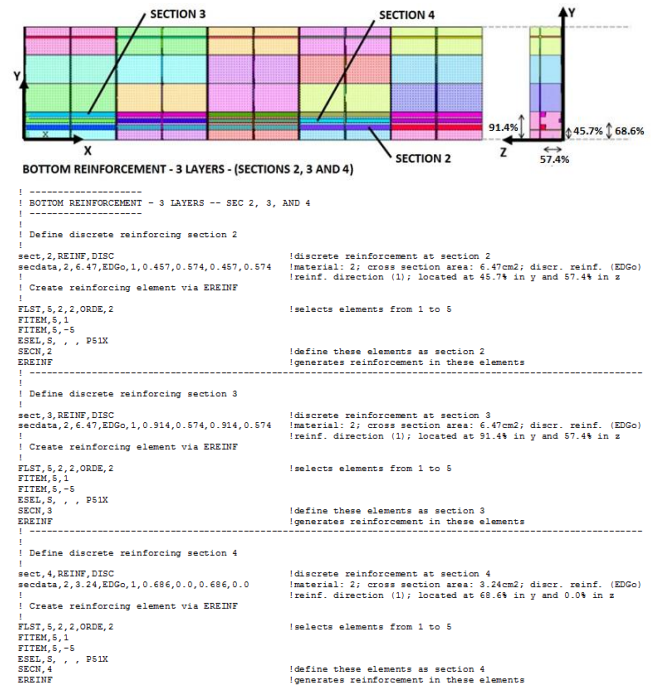


Fig. 6 Example of scripting with element REINF264 – Bottom rebars

reinforcing fibers in a volume. Each fiber, in this case, is independently modeled as a bar only with axial stiffness, allowing the specification of a number of reinforcing fibers in one base element. The nodal coordinates, degrees of freedom, and connectivity of element REINF264 are identical to those of the base element. Element REINF264 also allows the use of models for mechanisms such as plasticity, creep, initial stress, and large deformations. Incidentally, should a smeared type of modeling for the reinforcement be preferred, element REINF265 could be adopted, or even element REINF263, for plane stress states.

Element REINF264, therefore, has been chosen to represent the bonded reinforcing bars for the structure analyzed using the Element-Embedded Reinforcement model. This type of element has been also used to represent the bonded prestressing reinforcements through the same model. The finite element types that are compatible with element REINF264 are indicated in Fig. 4, where the twenty-node hexahedral element is highlighted.

Scripting is the most efficient method to add and discretize the reinforcement in ANSYS, which also facilitates the verification of possible mistakes. As an example of implementation through scripting, Fig. 6 shows, with comments, how the longitudinal bottom rebars of the beam indicated in Fig. 5 can be added to the model. It can be observed that the rebars have to be indicated in each finite element in a normalized fashion.

When unbonded tendons and cable-stays are considered, however, the element REINF264 is not used. In these cases, element LINK180, a unidimensional element with three degrees of freedom per node (X, Y, and Z translations), is used instead, avoiding any bonding of the tendons with the concrete. With this choice, however, the Element-Embedded Reinforcement model is unfortunately not

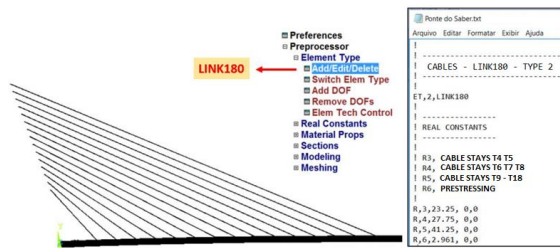


Fig. 7 Example of discretization with LINK180 elements

available and mesh constraints may be an issue. The tendons modeled in a discrete form with elements LINK180 have to have nodes coinciding with the nodes of elements SOLID186 of concrete, but, fortunately in the case herein, only at the anchorage points. Fig. 7 shows an example of script on how to add the data for the cable-stays and the diagonal tendons at the strengthened sections of the bridge.

4.2 Modeling the concrete

Additionally, to a variety of finite element types, ANSYS also presents a number of constitutive models to simulate the behavior of materials. Regarding concrete, for instance, there is an elastoplastic model with cracking consideration based on the rupture surface of five parameters by Willam and Warnke. The problem with this option, however, is that it can only be used with element SOLID65, which, in its turn, does not allow the use of the Element-Embedded Reinforcement model, but only the Discrete and the Smeared approaches. Although these approaches are perfectly fine options for modeling the reinforcement, only the Element-Embedded approach realistically and efficiently models the reinforcement. The reinforcement is not actually represented in a Smeared approach, while the Discrete option tends to demand finer meshes. An unnecessarily higher number of finite elements would only make numerical simulations slower, more difficult to solve due to convergence issues, and would demand machines with higher computational power. Therefore, since this work is about the structural analysis of the constructive phases of a cable-stayed segmental bridge that involves a considerable amount of finite elements and complex material behaviors, the Element-Embedded approach has been the one preferred. The implementation of this option, however, was only possible in ANSYS through its UPF customization tool (User Programmable Features).

Through the UPF customization tool of ANSYS, it was possible to implement numerically a new viscoelastoplastic material model with cracking consideration based on the rupture criterion by Ottosen (1977) to represent the concrete, as recommended by *fib* Model Code 2010 (2012). This new model for the concrete has been implemented in FORTRAN programming language in the subroutine USERMAT (User Material Routine).

In order to make the UPF system available for use, ANSYS has to be installed with the option “ANSYS Customization Files” activated, which automatically creates folders “Custom” and “Customize” in the path “C:\Program Files\ANSYS Inc\v145\ansys”. In this way, the subroutine

```

-----
! CONCRETE - USER - MATERIAL 200
!
! Constitutive model of user material
!
tb,user,200,1,6           ! Material ID:200, 1 temperature,
                          ! 6 constants(prop)
tbtemp,1,0              ! First temperature
tbdata,1,E1, v1, fc,1,212121.006,0 ! Temperature 1, E, Poisson, fc, aggregate,
! loading steps, initial date
tb,state,200,,9         ! Define 9 state variables

```

Fig. 8 Example of input data file

USERMAT can be accessed for new user implementations, compiling and linking it to the main program ANSYS. More specifically, in this work, the new model has been created inside the subroutine USERMAT3D, which is called by the subroutine USERMAT when three-dimensional elements are used. Incidentally, subroutine USERMAT contains three other subroutines that can be edited: USERMATPS, for elements under plane stress states; USERMATBM, for three-dimensional elements of the type BEAM; and USERMAT1D, for one-dimensional elements. Also, worth mentioning is that subroutine USERMAT is available for a family of 18 finite elements, such as: LINK180; SHELL181; PLANE182; PLANE183; SOLID185; SOLID186; SOLID187; BEAM188; and BEAM189 (ANSYS 2013).

Subroutine USERMAT is called in every Newton-Raphson iteration during a mechanical analysis in ANSYS. Additionally, stresses, displacements, and a number of variables are initially stored and then updated after each increment of time.

The input parameters that are necessary to the new constitutive model are given in the input data file by the command “TB, USER”. An example on how to use this command is presented in Figure 8. The command asks for six variables: modulus of elasticity; Poisson’s ratio; compressive strength; type of aggregate; loading steps; and initial date, with remaining data calculated internally.

Regarding the variable “aggregate”, there are internally available in USERMAT3D four aggregate types for calculation of the modulus of elasticity. The identification of each type is as follows: “1” for basalt; “2” for quartz; “3” for limestone; and “4” for sandstone aggregate.

The parameter “loading steps” regards two distinct procedures used to simulate the viscoelastoplastic behavior of concrete: STEP 1 and STEP 2. In STEP 1, the response of the structure with time is determined through an incremental process, where an interval of 1 day is considered herein. In this step, a viscoelastic behavior is adopted for the concrete, taking into consideration the effects of creep, shrinkage, and relaxation. In STEP 2, the equilibrium of the structure is reached after an increment of the instantaneous load. This step corresponds to a static state, where the elastoplastic behavior of the structure is analyzed.

In general, as many loading cases as wanted are allowed in the computational model, with the steps sequentially conducted in accordance with the specified loading dates. In the example presented in Fig. 8, the parameter that indicates the amount and sequence of steps is represented by the number 212121.006. The digits to the left of the dot



Fig. 9 Model BISO available in ANSYS

represent the sequence of steps, from right to left, while the digits to the right of the dot represent the amount of loading cases. Therefore, in the example, six steps are to be conducted in the following sequence: STEP 1 + STEP 2 + STEP 1 + STEP 2 + STEP 1 + STEP 2. The number of days of each STEP 1 is given through the variable “nsubst”, with the number of steps corresponding to the number of load increments that is indicated for each loading case in the input data script.

It is worth mentioning that more than one USERMAT3D material model can be specified in the input data script. In the analysis of the “Ponte do Saber” bridge, for instance, 16 different concrete USERMAT3D material models have been specified, with their initial date as the only difference between them. Incidentally, through the variable “initial date”, it is possible to indicate the exact time that the element is to be considered in the analysis. If the initial date were earlier than the current date (concrete pouring date), a very low stiffness would be considered for the respective elements, simulating deactivated elements. If an equal or a later date were considered, then the actual stiffness of the specified elements would be taken into consideration, simulating activated elements, and the analysis would be carried out according with the constitutive equations implemented in USERMAT3D. Through this control, the simulation of the constructive phases of the bridge analyzed herein has been carried out with no need of actual deactivations or activations of elements (also known as “birth/death” of elements), making a nonlinear analysis more stable.

4.3 Modeling of steel

The Element-Embedded Reinforcement model is the approach adopted in most part of the model due to the advantages and aspects already mentioned. The only exceptions are the cable stays and the diagonal post tensioned tendons that are modeled with elements LINK180.

In this work, two different constitutive models are used for the steel. The BISO model (Bilinear Isotropic Hardening), which is available in the internal library of ANSYS, is used for the reinforcing bars. However, a model that has been created through the UPF system with subroutine USERMAT1D is specified for the tendons and cables.

The bilinear constitutive model, BISO, is illustrated in Fig. 9. It can be seen that the initial slope of the stress-strain curve is the modulus of elasticity of the material, E . Then, after reaching the yield stress, σ_0 , the diagram continues

```

-----
! REINFORCEMENT - USER - MATERIAL 2
-----
! Constitutive model of user material
-----
!
tb,user,2,2,5           ! Material ID:2, 2 temperatures,
                       ! 5 constants (prop)
tbtemp,1,0             ! First temperature
tbdata,1,20500,0.3,179,96,28 ! Temperature: 1, E, Poisson, Fptk,
                       ! prestressing tension, date of prestressing
tb,state,1,,9          ! Define 9 state variables

```

Fig. 10 Example of input data script for prestressing steel model

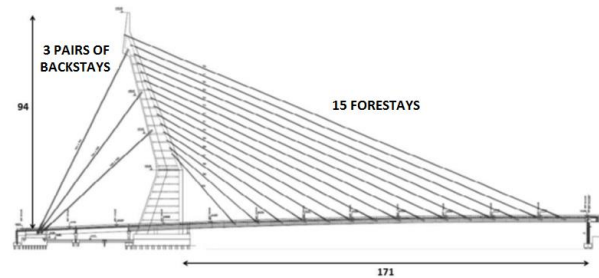


Fig. 11 Elevation view of the “Ponte do Saber” bridge (GARAMBONE 2012)

along a line with a slope that identifies a tangent modulus, specifying the hardening modulus, E_T . This value cannot be neither negative nor bigger than the specified modulus of elasticity.

Another model has also been implemented through subroutine USERMAT1D to calculate the initial stresses for the prestressing tendons and cables. Using this resource, the numerical implementation of the model with time dependent properties has been carried out to consider relaxation effects for the prestressing steel, as recommended by *fib* Model Code 2010 (2012). An example of input data script for this model, using once again the command “TB, USER”, is presented in Fig. 10.

Subroutine USERMAT1D can also be used as many times as need and, specifically for “Ponte do Saber” bridge, 15 material instances are specified in USERMAT1D to represent the 15 forestays. Therefore, each forestay is specified by its cross-section area and, very importantly, its initial prestressing date. This information is critical for an adequate calculation of the time dependent effects that tend to occur along the constructive steps of the structure.

5. Numerical simulation of the bridge

The “Ponte do Saber” bridge has been chosen for this study because of all the data available in the Master’s thesis by Gomes (2013) and in the thesis by Toledo (2014). These works present in detail data about the bridge’s geometry, materials used, as well as describe each of its constructive phases. Therefore, design and modeling information, analysis steps (load cases) and comments on the obtained results can be appropriately given as follows.

5.1 Information about the bridge

The “Ponte do Saber” bridge was opened in 2012 in Rio

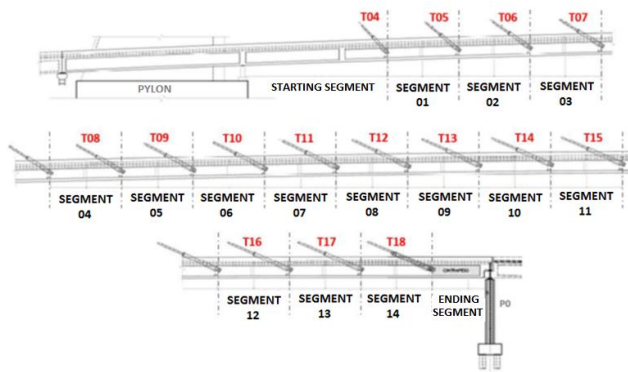


Fig. 12 Location of forestays along the box girder (GARAMBON 2012)

Cable stay	Number of strands	Steel cross section (cm ²)	Cable stay	Number of strands	Steel cross section (cm ²)
T01	127 ϕ	190.5	T10	55 ϕ	82.5
T02	127 ϕ	190.5	T11	55 ϕ	82.5
T03	127 ϕ	190.5	T12	55 ϕ	82.5
T04	31 ϕ	46.5	T13	55 ϕ	82.5
T05	31 ϕ	46.5	T14	55 ϕ	82.5
T06	37 ϕ	55.5	T15	55 ϕ	82.5
T07	37 ϕ	55.5	T16	55 ϕ	82.5
T08	37 ϕ	55.5	T17	55 ϕ	82.5
T09	55 ϕ	82.5	T18	55 ϕ	82.5

Fig. 13 Number of strands and steel cross section area for each cable stay (GOMES 2013)

de Janeiro city and is one of the routes to a demanding traffic at the “Cidade Universitária” (University City) region. This region is in the Federal University of Rio de Janeiro area, UFRJ, accessing the “Presidente João Goulart” expressway (also known as “Linha Vermelha”, or the “Red Line”). The bridge presents 170.46 m in its main span, with a pylon measuring 94 m in height. Fig. 11 shows an elevation view of the bridge.

The “Ponte do Saber” bridge is composed of 21 cable stays, with 6 of them comprising three pairs of backstays, while 15 are forestays spaced at every 10m along the longitudinal axis of the deck and at every 4m along the height of the pylon (tower). The backstays counterbalance the addition of new box segments longitudinally, tensioning the forestays and bending the geometric axis of the pylon inward during the bridge’s construction.

The pairs of backstays are numbered from T01 to T03, while the forestays are numbered from T04 to T18. The arrangement of the forestays along the bridge’s deck is shown in Fig. 12, with T04 as the nearest to the pylon and anchored approximately at 21 m from its edge.

The prestressing strands used in the bridge are composed of seven galvanized wires classified as type CP-177RB (Brazilian code NBR7483), having a nominal diameter of 15.7 mm. The amount of strands at the anchorage points vary from 31 to 127, with the latter specified for the backstays and the former (also 37 and 55 strands) for the forestays. The number of strands and the steel cross section in each cable stay is summarized in Fig. 13.

The forces in the tendons are likely to suffer considerable variations with the ongoing stay prestressing sequence. This is mainly because of the deck’s slenderness, which tends to induce large deflections when either a box

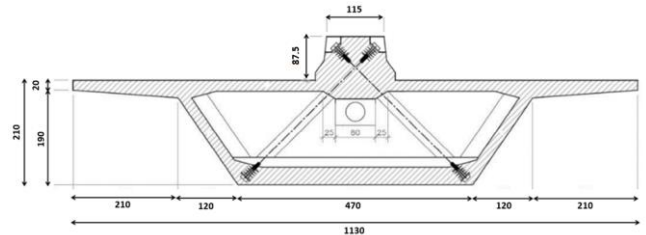


Fig. 14 Cross section of the bridge (GARAMBONE, 2012) – dimensions in cm

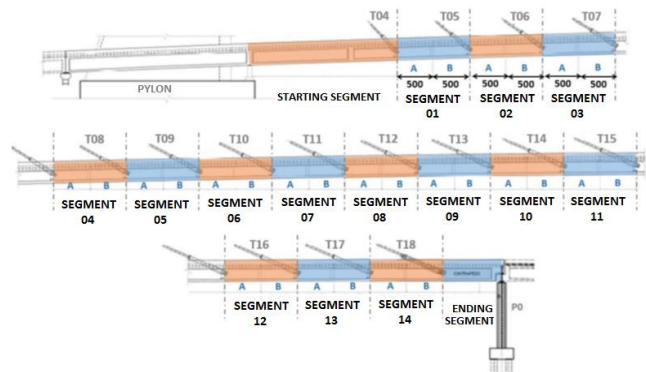


Fig. 15 Positions of the segments along the main span of the bridge (GARAMBONE 2012)

segment is added or a stay tendon is prestressed. In the case of the “Ponte do Saber” bridge, the prestressing of the cable stays and their forces in every constructive phase have been monitored with load cells. The data have been recorded and the monitoring of the bridge is an ongoing task to be carried out along its service life. The recorded field data from this monitoring is important not only for comparisons with estimated design parameters, but also for validation of the numerical results obtained in this work.

Reinforced concrete box segments comprise the cross sections of the “Ponte do Saber” bridge. Its deck measures a total width of 11.3 m and a total height of 2.1 m, as can be seen in Fig. 14. The concrete is designed for a compressive strength of 50 MPa, but simple compression tests in the lab have indicated a mean strength of 69 MPa.

The cross section of the bridge presents a longitudinal central beam for added stiffness. Additionally, lateral cantilevers measuring 210 cm in length and from 20 to 35 cm in thickness are also present. The inner cell of the box section presents thicknesses of 22 cm in most part of the top slab and of 35 cm at the bottom slab, presenting also two lateral inclined webs with a thickness of 22 cm.

The positions of the 16 box segments along the longitudinal axis of the bridge are illustrated in Fig. 15. The ending segment has a different length, when compared with the other 14 segments composed by type A and type B parts, each measuring 5 m. Pier P0 is located at the far end from the bridge’s pylon, working as a support for the ending box segment. It is important to comment that the connection between the bridge’s girder and the pylon can be considered as monolithic, since there are no bearings between these two structural elements.

A diagonally pre-tensioned W-shaped strengthening



Fig. 16 Internal view of a strengthening W-section (GOMES 2013 and TOLEDO 2014)



Fig. 17 Cast in place segmental cantilever method (GARAMBONE 2012)

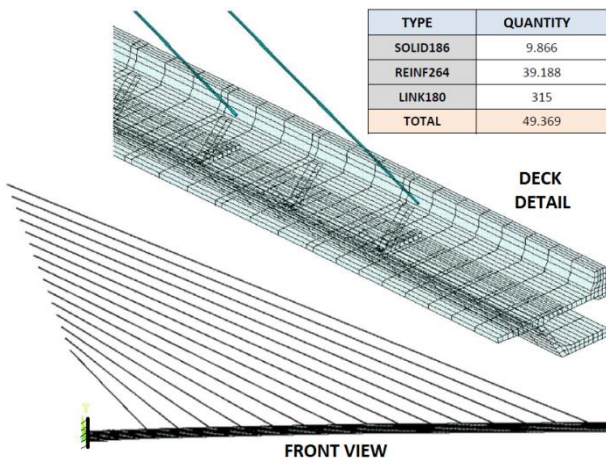


Fig. 18 ANSYS model and the numbers and types of finite element used

section (PWS – Prestressed W Section) has been designed at the final 35 cm of every type-B segment part. This

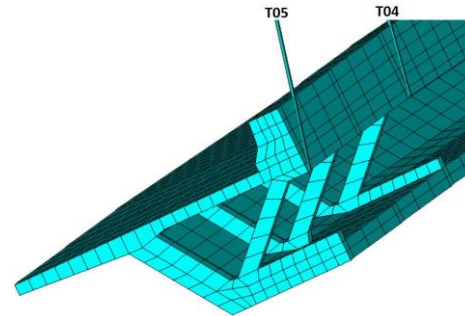


Fig. 19 Model view of the starting segment, segment 01, strengthened sections and cable stays

section is composed of two inclined webs and two inclined ties, with the latter responsible to transmit the reaction from the stiffening beam to the load application point of a cable stay. Each tie is pre-tensioned with tendons of twelve 12.7 mm-diameter strands.

A W-shaped strengthening section is also designed for the final 35 cm of every type-A segment part, working without any prestressing (RWS – Reinforced W Section). An internal view of the bridge showing a W-shaped strengthening section is presented in Fig. 16.

The cast in place segmental cantilever method has been the option chosen to erect the “Ponte do Saber” bridge, with box segments cast in place to allow the construction of the pylon in parallel with the cable stay prestressing sequence. Fig. 17 shows the ongoing construction of the bridge.

The starting segment, which is localized between the edge of the pylon and stay cable T04, has been completely strutted for its concrete casting. The following segments, however, have been erected according with the sequence below: casting in place of type-A segment part (5 m in length); formwork is pushed over type-A segment part; casting in place of type-B segment part (5 m in length); prestressing of tendons in PWS section; prestressing of cable stay; and formwork is pushed over type-B segment part.

5.2 Modeling of the bridge

Because of the size of the problem to be solved, the numerical model of the “Ponte do Saber” bridge is developed in this work only with the consideration of the main span and the forestays. Therefore, the pylon, the backstays, and the smaller span are not considered in the modeling. Reducing even further the number of finite elements needed, the transversal symmetry of the bridge is also used, allowing the consideration of only half of the structure. Fig. 18 shows an elevation view and a highlighted detail of the final model.

Concrete elements are modeled with SOLID186, reinforcing bars with REINF264, while cable stays and prestressing tendons with LINK180 elements. Regarding the boundary conditions, the nodes shared between the pylon and the top ends of the cable stays, as well as at the contacts with the girder are considered fixed. The amount of each type of finite element used in the numerical model can be seen in the table shown in Fig. 19.

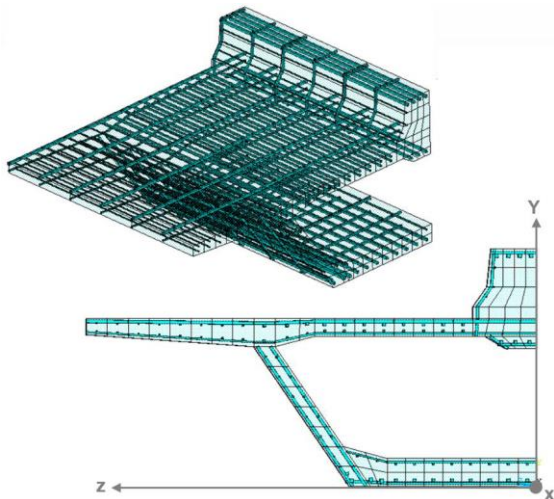


Fig. 20 View of the longitudinal and the transversal rebars of the model

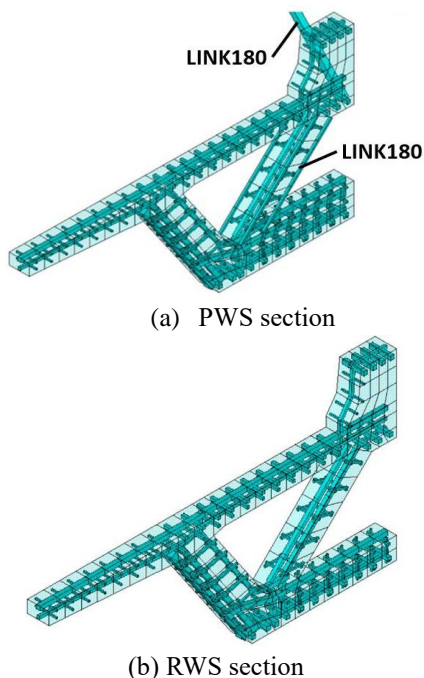


Fig. 21 Discretization of reinforcement in strengthened sections

The new viscoelastoplastic rheological model that has been implemented in subroutine USERMAT3D is used to model the behavior of the concrete. Poisson's ratio is considered as 0.2, while the compressive strength of the concrete is adopted as 69 MPa. Additionally, a basaltic aggregate is considered in the model.

After modeling the box segments using concrete's finite elements, an elastic linear test is carried out to verify the effectivity of the connection among the nodes. The next step is, by following the drawing plants, which is available in Garambone (2012), the modeling of the rebars with REINF264 elements and the Element-Embedded Reinforcement model. A view of the longitudinal and the transversal rebars in a standard cross section of the bridge is illustrated in Fig. 20.

Figs. 21(a) and 21(b) show the mesh for the reinforcement used in section types PWS and RWS, respectively. Specifically, in Fig. 21(a), elements LINK180 for the stays and for the diagonal prestressing tendons are shown. Regarding the stays, displacements are imposed at their top nodes connecting to the pylon, producing the desired design slope.

5.3 Analysis steps

The analysis is divided into 78 load cases to simulate numerically the construction phases of the "Ponte do Saber" bridge. Overall, the starting segment, the ending segment, and the fourteen 10 m-long segments in between present the following constructive sequence:

- a) STEP 1: analysis of the time dependent effects during casting of the segments;
- b) STEP 2: consideration of the segment's dead load (DL) and the weight of the formwork on the next segment, removing it from the previous one, if existent;
- c) STEP 2: prestressing of the cable stay located at the end of the segment. This prestressing is carried out by imposing a displacement at the node supposedly attached to the pylon;
- d) STEP 1: a time increment of 1 day is applied to the prestressed diagonal tendons and to the stay in the previous step. This increment is needed since the prestressing model is activated only in a STEP 2. Therefore, to avoid convergence difficulties, the prestressing activation step is considered separately, after the displacement imposition is applied in the stay;
- e) STEP 2: the prestressing model is activated and the time dependent effects of the materials are taken into consideration from the specified time date forward.

5.4 Analysis of results

In Figs. 22 to 29 are indicated graphs with span deflections along the main constructive phases of the "Ponte do Saber" segmental bridge, i.e., the results for the load cases of dead load of segments and for the load cases when stays in segments 04, 07, 10, and 13 are prestressed.

It can be observed that the curve obtained numerically with ANSYS is slightly below the design slope (Grade) in the cases when the dead load of the segments is applied, getting closer or even above the design values when the stays are prestressed. Considering the monitored field data, during the initial phases, there is an agreement with the Grade curvature after application of the dead load, getting above the Grade just after stay prestressing.

After the load case that corresponds to the application of the dead load of segment 07, it can be observed that the field data is above the Grade, during both steps of dead load and stay prestressing considerations.

The cable stay prestressing process is simulated numerically so that the bridge's deck returns to the designed Grade slope after the imposition of a displacement at the top end of each cable stay. This procedure showed to be adequate, resulting in data that agree with the results obtained originally for the bridge.

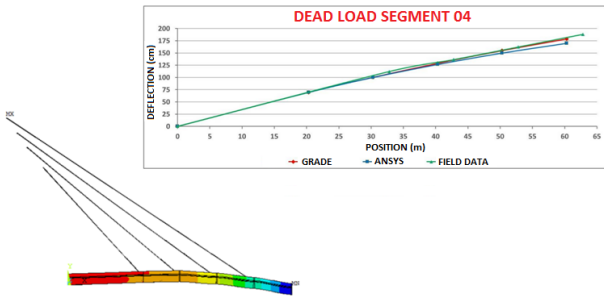


Fig. 22 Deformed shape and position vs. deflection diagram – Dead load of segment 04

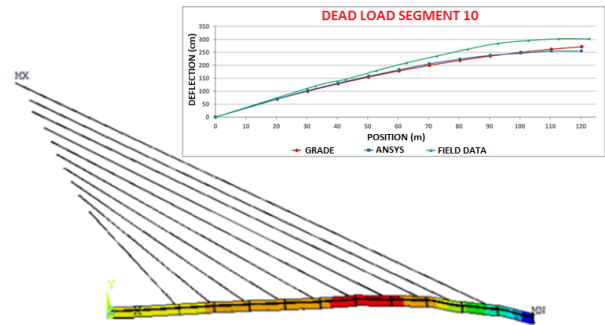


Fig. 26 Deformed shape and position vs. deflection diagram – Dead load of segment 10

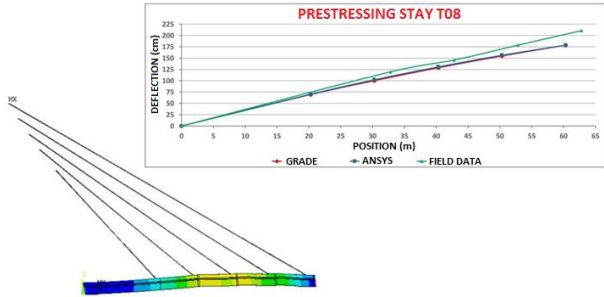


Fig. 23 Deformed shape and position vs. deflection diagram – Prestressing of stay T08

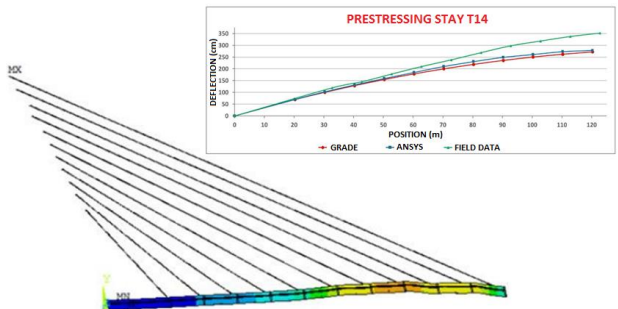


Fig. 27 Deformed shape and position vs. deflection diagram – Prestressing of stay T14

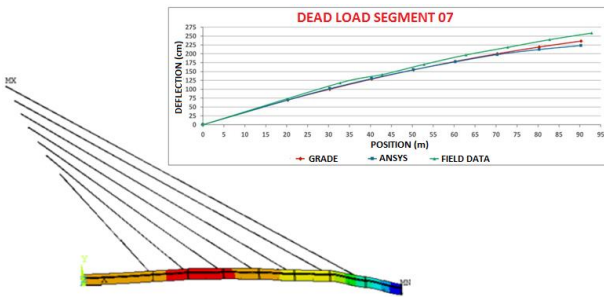


Fig. 24 Deformed shape and position vs. deflection diagram – Dead load of segment 07

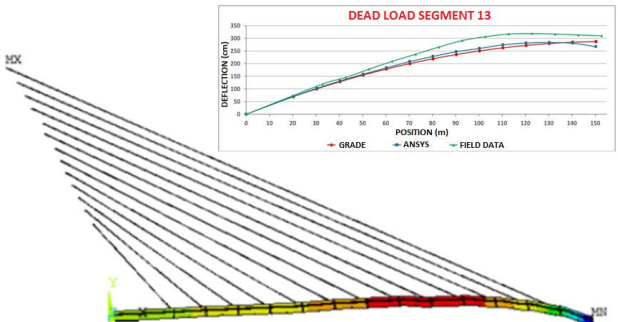


Fig. 28 Deformed shape and position vs. deflection diagram – Dead load of segment 13

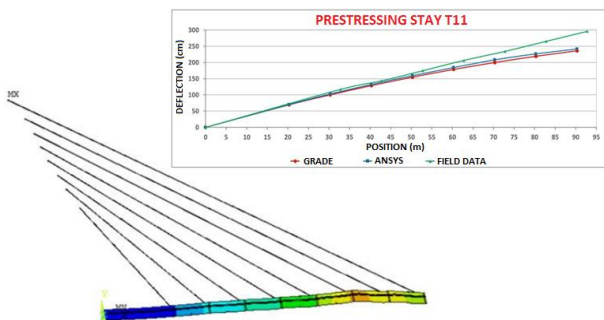


Fig. 25 Deformed shape and position vs. deflection diagram – Prestressing of stay T11

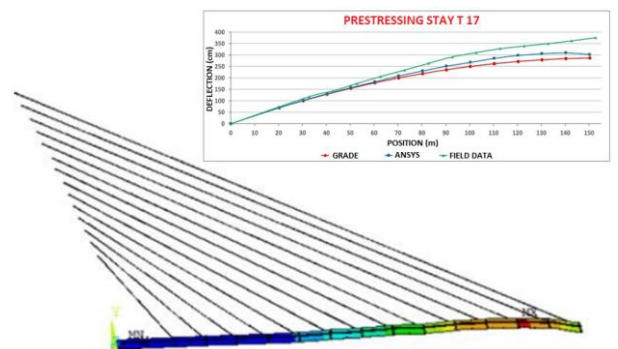
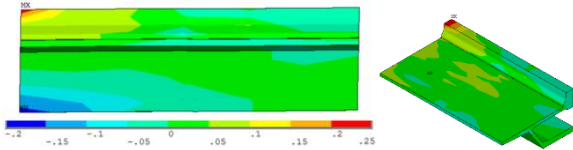


Fig. 29 Deformed shape and position vs. deflection diagram – Prestressing of stay T17

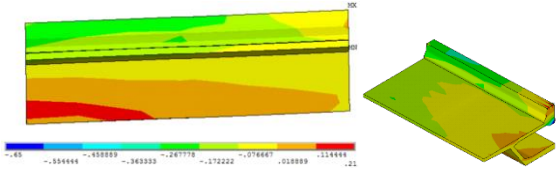
When analyzing creep effects, it is observed that they are not as important as originally estimated in the design. This is probably because regions of concrete elements are subjected to alternating tension and compression forces during the construction. This situation differs considerably from when only compressive action is present, which tends to produce creep effects considerably higher.

Since the analysis has generated a very large amount of data, only some of the most relevant results are presented as follows. Specifically, in Fig. 30, the stresses in the concrete of segment 01 are presented for the following load cases:

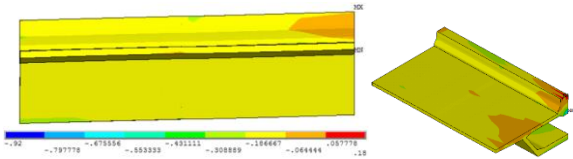
SEGMENT 01 – DEAD LOAD OF SEGMENT 01 – 81 DAYS



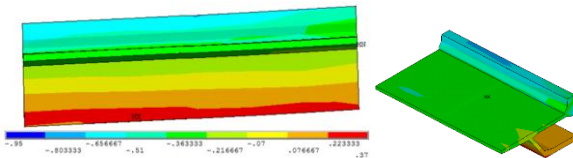
SEGMENT 01 – PRESTRESSING OF STAY T05 – 81 DAYS



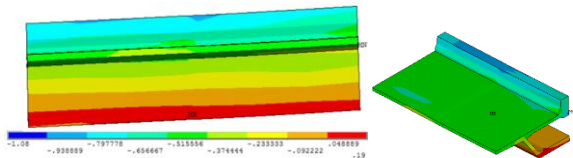
SEGMENT 01 – DEAD LOAD OF SEGMENT 04 – 117 DAYS



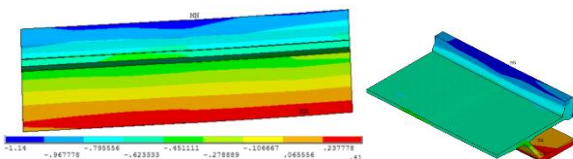
SEGMENT 01 – PRESTRESSING OF STAY T08 – 117 DAYS



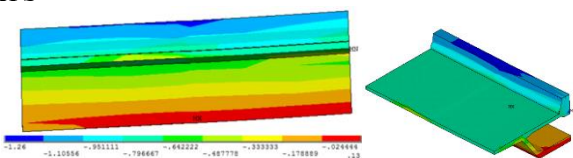
SEGMENT 01 – DEAD LOAD OF SEGMENT 08 – 166 DAYS



SEGMENT 01 – PRESTRESSING OF STAY T12 – 166 DAYS



SEGMENT 01 – DEAD LOAD OF SEGMENT 12 – 232 DAYS



SEGMENT 01 – PRESTRESSING OF STAY T16 – 232 DAYS

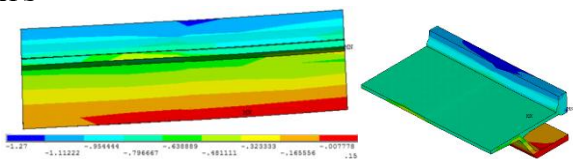
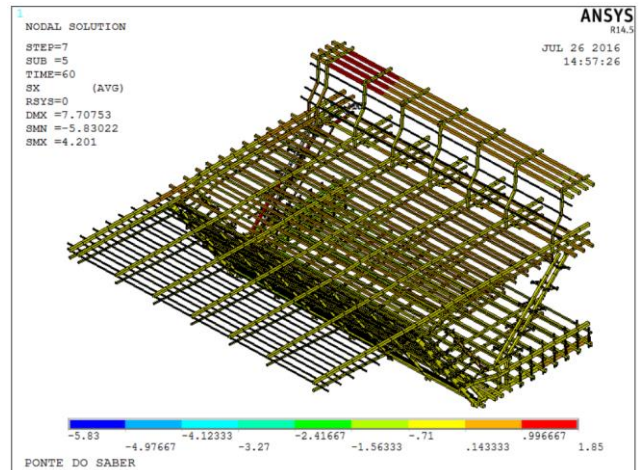


Fig. 30 Concrete stresses σ_x (kN/cm²) – Segment 01

SEGMENT 01 – DEAD LOAD OF SEGMENT 01



SEGMENT 01 – PRESTRESSING OF STAY T05

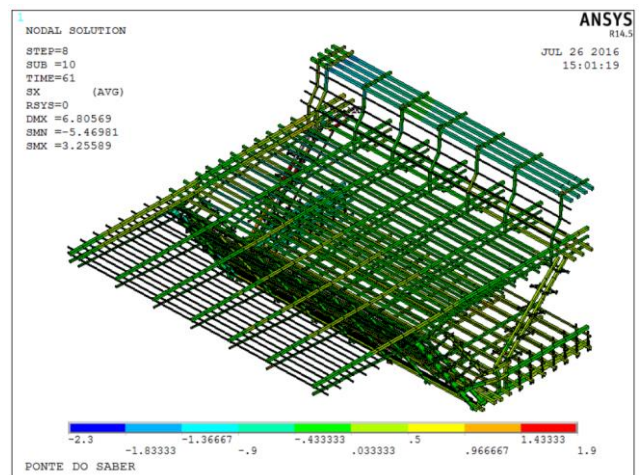


Fig. 31 Stresses in rebars (kN/cm²) – Segment 01

dead load of segment 01; prestressing of stay T05; dead load of segment 04; prestressing of stay T08; dead load of segment 08; prestressing of stay T12; dead load of segment 12; and prestressing of stay T16. In these results, the concrete presents tension stresses on the top surface of the cross sections when the dead load of the structure is applied. Nevertheless, upon prestressing the cable stays, the stresses invert, occurring tension stresses on the bottom surface. This effect can be easily noticed in the first load cases. As the formwork is moved forward, the stresses tend to be stabilized as compression on the top surface and as tension on the bottom. Additionally, as expected, when the concrete of the segments ages, the material becomes increasingly stronger.

Fig. 31 shows rebar stresses along the first 5 m of segment 01. It can be observed that, when the segment's dead load is applied, its top rebars become tensioned. Nevertheless, when the prestressing of cable stay T05 occurs, compressive stresses are then observed in the top rebars.

An evolution of stresses for stays T04 and T08 is presented in Figs. 32 and 33. The curves shown are drawn from the following sources: the results obtained with the ANSYS model, the estimated stresses given originally, and

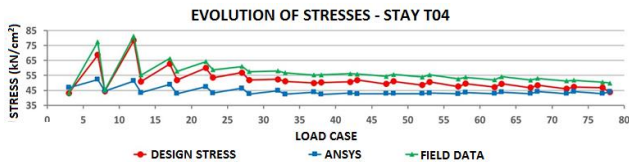


Fig. 32 Load case vs. stress – cable stay T04

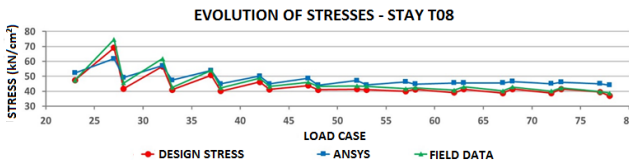


Fig. 33 Load case vs. stress – cable stay T08

from monitored field data. These graphs show that, in general, the stresses suffer larger variations during initial phases, becoming more stable as the construction advances. When dead loads are applied, higher stresses are observed in the stays, when compared with the previous stay prestressing phase. Additionally, both curves obtained from field data and from the original design present reasonable agreement with the curve obtained numerically.

6. Conclusions

Results for the construction phases of a segmental bridge that is carried out numerically with a model implemented in ANSYS are compared with field data monitored during the bridge's construction and with original estimations made during design. The comparison showed good agreement, highlighting how important stresses developed during the construction of such type of structure can be, where the Cast in Place Segmental Cantilever Method is used. The cross sections must have enough strength to endure the tensile and the compressive stresses that are produced during the casting in place of the box segments and the prestressing of the cable stays. The data indicates an important difference between the slopes (Grade) gathered in the field and the estimated values during the design of the bridge. This difference may be explained by the use of simplified processes adopted during the design to account for time dependent effects (creep of the concrete and relaxation of the steel). It can be observed that the bridge's Grade is overestimated, relatively to designed values. This may result in considerable elevation gaps at the ending segment between the deck and its supporting column or abutment.

Acknowledgments

The authors wish to acknowledge the financial support given by the Civil Engineering Graduate Program – PPGEC of the Federal University of Rio Grande do Sul – UFRGS, and by the Brazilian governmental research institutions CAPES and CNPq.

References

- Adiyaman, G., Yaylaci, M. and Birinci, A. (2015), "Analytical and finite element solution of a receding contact problem", *Struct. Eng. Mech.*, **54**(1), 69-85.
- Amiri, G.G., Jahromi, A.J. and Mohebi, B. (2012), "Determination of plastic hinge properties for static nonlinear analysis of FRP-strengthened circular columns in bridges", *Comput. Concrete*, **10**(5), 435-455.
- Anil, Ö. and Uyaroglu, B. (2013), "Nonlinear finite element analysis of loading transferred from column to socket base", *Comput. Concrete*, **11**(5), 475-492.
- ANSYS (2013), *Inc. Theory Reference (Version 14.5)*.
- Bulut, N., Anil, Ö. and Belgin, C.M. (2011), "Nonlinear finite element analysis of RC beams strengthened with CFRP strip against shear", *Comput. Concrete*, **8**(6), 717-733.
- Chen, W.F. and Han, D.J. (1988), *Plasticity for Structural Engineers*, Springer-Verlag, New York, U.S.A.
- Comité Euro-International du Béton (2012), *CEB-FIP Model Code 2010*, Bulletin N. 65.
- Demir, A., Tekin, M., Turali, T. and Bagci, M. (2014), "Strengthening of RC beams with prefabricated RC U cross-sectional plates", *Struct. Eng. Mech.*, **49**(6), 673-685.
- Demir, S. and Husem, M. (2015), "Investigation of bond-slip modeling methods used in FE analysis of RC members", *Struct. Eng. Mech.*, **56**(2), 275-291.
- Garambone, V.F. (2012), *Ponte do Saber*, Paper Presented during the V Brazilian Congress of Bridges and Structures.
- Gomes, R.R.S. (2013), "Technical and constructive considerations of a cable stayed bridge design", M.Sc. Dissertation, Federal University of Rio de Janeiro, Rio de Janeiro, RJ, Brazil.
- Hinton, E. (1988), *Numerical Methods and Software for Dynamic Analysis of Plates and Shells*, Pineridge Press Limited, Swansea, Wales, U.K.
- Kazaz, I. (2011), "Finite element analysis of shear-critical reinforced concrete walls", *Comput. Concrete*, **8**(2), 143-162.
- Kibar, H. and Ozturk, T. (2014), "The evaluation with ANSYS of stresses in hazelnut silos using Eurocode 1", *Struct. Eng. Mech.*, **51**(1), 15-37.
- Lazzari, B.M., Campos Filho, A., Lazzari, P.M. and Pacheco, A.R. (2017a), "Using element-embedded rebar model in ANSYS for the study of reinforced and prestressed concrete structures", *Comput. Concrete*, **19**(4), 347-356.
- Lazzari, B.M. (2015), "Finite element analysis of reinforced and prestressed concrete elements under plane stress states", M.Sc. Dissertation, Federal University of Rio Grande do Sul, Porto Alegre, RS, Brazil.
- Lazzari, P.M. (2016) "Numerical simulation of construction stages of cable-stayed bridges through the finite element method", Ph.D. Dissertation, Federal University of Rio Grande do Sul, Porto Alegre, RS, Brazil.
- Lazzari, P.M., Campos Filho, A., Lazzari, B.M. and Pacheco, A.R. (2017b), "Structural analysis of a prestressed segmented girder using contact elements in ANSYS", *Comput. Concrete*, **20**(3), 319-327.
- Mondal, T.G. and Prakash, S.S. (2016), "Nonlinear finite-element analysis of RC bridge columns under torsion with and without axial compression", *J. Brid. Eng.*, **21**(2), 04015037.
- Ottosen, N.S. (1977), "A failure criterion for concrete", *J. Eng. Mech. Div.*, **103**(4), 527-535.
- Shaheen, Y.B.I., Mahmoud, A.M. and Refat, H. (2016), "Structural performance of ribbed ferrocement plates reinforced with composite materials", *Struct. Eng. Mech.*, **60**(4), 567-594.
- Toledo, R.L.S. (2014) "Design of cable-stayed bridges concrete stiffening girders", M.Sc. Dissertation, Federal University of Rio de Janeiro, Rio de Janeiro, RJ, Brazil.
- Zhu, Q., Xu, Y.L. and Xiao, X. (2015), "Multiscale modeling and

model updating of a cable-stayed bridge. I: Modeling and influence line analysis”, *J. Brid. Eng.*, **20**(10), 04014112.

CC